JOURNAL OF MATERIALS SCIENCE **34** (1999) 5005–5013

Phase formation, sintering behavior, and electrical characteristics of NASICON compounds

HEE-BOG KANG*
Ceramic research Div., Korea Institute of Sci. and Tech., Seoul, Korea

N.-H. CHO‡
Dept. of Ceramic Engineering, Inha University, Incheon, Korea
E-mail: nhcho@dragon.inha.ac.kr

The dependence of phase formation, sintering behavior, and electrical characteristics of Sodium Superionic Conductor (NASICON) compounds on sintering temperature, time, and cooling process was investigated. In the von Alpen-type composition $Na_{3.2}Zr_{1.3}Si_{2.2}P_{0.8}O_{10.5}$, ZrO_2 second phase is in thermal equilibrium with crystalline NASICON and liquid phase above 1320 °C, and when cooled through 1260–1320 °C, the crystalline NASICON was formed by reaction between the ZrO_2 second phase and the liquid phase. Maximum relative densities of 96 and 91% were obtained for compositions $Na_3Zr_2Si_2PO_{12}$ and $Na_{3.2}Zr_{1.3}Si_{2.2}P_{0.8}O_{10.5}$, respectively. For these compositions, the maximum ionic conductivity and the minimum migration barrier height were 0.45 $ohm^{-1}\,cm^{-1}$ and 0.07 eV, respectively. The migration barrier height of the high temperature form (space group: R3c) is about 30–40% of that of the low temperature form (space group: C2/c). Ionic conductivity increases with increasing sinterability, and a considerably large amount of glass phase in $Na_{3.2}Zr_{1.3}Si_{2.2}P_{0.8}O_{10.5}$ ceramics significantly lowers ionic conductivity above the transition temperature.

1. Introduction

Sodium superionic conductor (NASICON) has attracted scientific and technological attention for the last decade, especially in view of its technical applications in energy-related or environmental fields [1, 2]. This is mainly due to its promising electrical properties suitable for gas sensors and energy storage systems [3–7]. Various battery systems have been developed to provide propulsion energy for electric vehicles or to store excessive electrical energy of power plants to supply it when necessary. Na-S batteries, having high energy storage capacity and power compared with other battery systems, have been regarded as one of the potential candidates for such applications [3]. In order to be used as solid electrolytes for the Na-S battery system, the electrolytes should have high ionic conductivity, chemical stability with liquid electrodes, high mechanical strength and resistivity against degradation after operation [8–10].

NASICON has some useful and unique characteristics such as low sintering temperature, three dimensional framework, and considerably good ionic conductivity compared to other solid electrolytes particularly β-alumina [8, 9]. Though β-alumina has attracted much attention for the application as solid electrolytes in the Na-S battery system since it was developed by Weber *et al*, it has a layer structure, and as a result exhibits anisotropic characteristics in thermal expansion and electrical conductivity, causing mechanical failure after operation for a few hours [11–13].

NASICON with a chemical formula of $Na_{1+x}Zr_2Si_xP_{3-x}O_{12}$ $(0 < x < 3)$ was first reported by Hong *et al*. The skeleton of this compound consists of ZrO_6 octahedra, PO_4 tetrahedra, and SiO_4 tetrahedra, and this compound has been reported to exhibit a few crystalline forms depending on temperature and composition (x), and most sintered NASICON contain certain amount of ZrO_2 second phases [14–16]. Unfortunately, the ZrO_2 has a monoclinic/tetragonal phase transition at 1100 °C, below the usual sintering temperatures of the NASICON compounds [17]. The monoclinic/rhombohedral phase transition of crystalline NASICON around 200 °C causes a dilatometric anomaly unfavorable for applications [18–21]. As a way of overcoming such technical problems, various compositional modifications have been reported by von Alpen, H. Kohler, S. Fujitsu *et al.* to improve its microstructure and physical properties [17, 18, 22, 23]. The von Alpen-type NASICON is of a ZrO_2 deficient form of the Hong's NASICON with a general formula of $Na_{1+x}Zr_{2-x/3}Si_xP_{3-x}O_{12-2x/3}$, containing little ZrO_2 second phase [17]. However, the correlation of

* *Current address*: Dept. of electrical communication engineering, Tohoku Univ., Tohoku, Japan.
‡ Author to whom all correspondence should be addressed.

crystalline NASICON phase formation, sintering behavior, and electrical conductivity of the compounds with synthesis techniques and sintering parameters has been rarely reported [24–29].

In this study, we try to elucidate the effect of sintering temperature, time and cooling processes on the formation of phases like the ZrO_2 and the crystalline NASICON, sintering behavior, and electrical characteristics for two NASICON compositions of $Na_3Zr_2Si_2PO_{12}$ and $Na_{3.2}Zr_{1.3}Si_{2.2}P_{0.8}O_{10.5}$. These compositions are one of the Hong-, and von Alpen-type NASICON, respectively, and, in this paper, referred to as H- and A-type composition, respectively. Complex impedance analysis was used to measure the electrical conductivity of the compounds. Migration loss of Na^+ ions was observed at a few MHz, and ionic conductivity was determined in a frequency-insensitive dc-conductive region below the loss frequency [30, 31]. The conductivity was measured at various temperatures below 300 °K, and migration barrier heights were determined from the variation of conductivity with temperature.

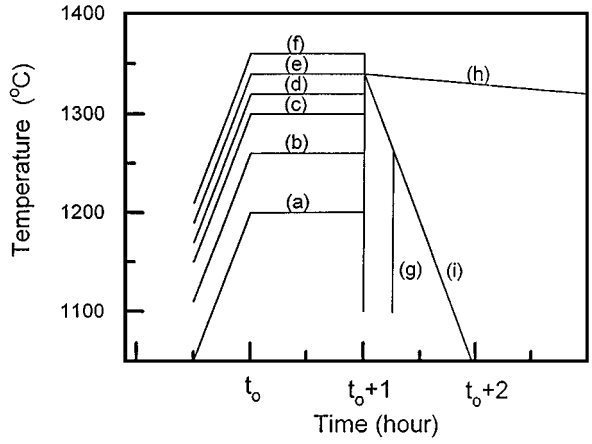

Figure 1 Sintering temperatures and cooling paths for the investigated samples. The samples were sintered at (a) 1200 °C, (b) 1260 °C, (c) 1300 °C, (d) 1320 °C, (e) 1340 °C, and (f) 1360 °C for 1 h, respectively, followed by air quench. Some samples were sintered at 1340 °C for 1 h and then either (g) furnace-cooled to 1260 °C or (h) cooled at 1 °C/h to 1260 °C, followed by air quench. Cooling path (i) indicates furnace-cooling to room temperature after sintering at 1340 °C for 1 h. The furnace-cooling rate is about 5 °C/min.

2. Experimental

2.1. Calcination and sintering

Starting materials used in the preparation of NASICON compounds were highly pure Na_2CO_3 (Aldrich Chemical Co., 99%), $Na_3PO_412H_2O$ (Kanto Chemical Co., extra pure), ZrO_2 (Aldrich Chemical Co., 99%), and SiO_2 (Hayashi Chemical Co., Guaranteed reagent). These materials were dried at 120 °C for 12 h, and then mixed in a polyethylene jar for 2 h according to the stoichiometric ratio for H- and A-type compositions. ZrO_2 balls and ethanol were used as mixing agents and mixing media, respectively.

NASICON phase formation was examined for the mixtures calcined at 1000°–1250 °C by X-ray diffractometry (XRD), and based on these results, appropriate calcination conditions for H- and A-type composition were 1150 and 1250 °C for 10 h, respectively [29]. The calcined powders were ball-milled for 30 h, and the dried powders were pressed into tablets under a pressure of 1000 kg/cm^2.

To investigate the effect of sintering temperature, the pressed tablets were sintered from 1160 to 1360 °C for 1 h on platinum foil in air atmosphere. Fig. 1 shows the various sintering and cooling procedures. To analyze the sintering mechanism, the pressed tablets of H- and A-type composition were sintered at 1280 °C for 1–16 h, and at 1300 °C for 0.5–4 h, respectively.

2.2. Physical property measurements

The density of sintered bodies was measured by Archimedes principle. Phases present in the calcined or sintered bodies were determined by X-ray diffraction techniques (Philips, ADP1700) using CuK_α radiation with Ni filter in a diffraction angle range of 10° to 40°. The microstructure and chemical composition of the compounds was analyzed by scanning electron microscopy (SEM, Hitachi, X-650) with an energy dispersive spectrometry (EDS) system. To measure electrical conductivity, the flat surfaces of the sintered tablets were prepared by polishing with successively finer grades of Al_2O_3 powders followed by diamond pastes down to 1 micrometer. Silver paste was applied as electrodes on both flat sides of the tablets. Conductivities were measured with an impedance/gain-phase analyzer (HP 4194A) in a frequency range of 10^2 to 4×10^6 from room temperature to 300 °C. A simple electrically heated furnace was employed. Nitrogen gas was circulated inside the furnace and the temperature was measured with chromel-alumel thermocouples in contact with the electrode. A schematic of the measurement system is shown in Fig. 2.

3. Results and discussions

3.1. NASICON phase formation

XRD curves in Fig. 3 were obtained from A-type samples, sintered at 1200, 1260, 1300, 1320 and 1360 °C for 1 h, respectively, and then air-quenched to room temperature. All the peaks correspond to either monoclinic NASICON or ZrO_2 phases. The ZrO_2 peaks are indicated with arrows. Spectra (b) and (c) consist of only the crystalline NASICON. However, spectra (d) and (e) show that the samples sintered above 1320 °C contain certain amount of ZrO_2 second phase. As all the samples were made by air quench after sintering, it is believed that considerable amount of ZrO_2 is in thermal equilibrium with the crystalline NASICON at 1340 °C.

In order to investigate the formation of the crystalline NASICON as well as the existence of the ZrO_2 phase when cooled through 1260–1300 °C, two different cooling paths were employed. First, in samples sintered at 1340 °C for 1 h and then furnace-cooled to 1260 °C, followed by air quench to room temperature, the amount of ZrO_2 second phase decreases significantly as shown in Fig. 4d. This indicates that a peritectic type reaction between the crystalline NASICON and the ZrO_2 occured around 1320 °C as shown in the reaction equation below.

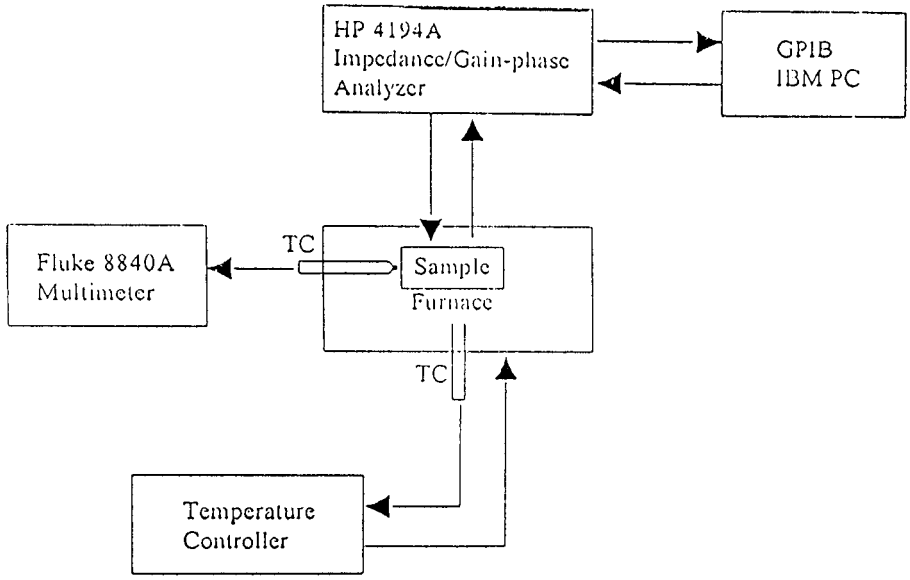

Figure 2 Schematic representation for the conductivity measurement system.

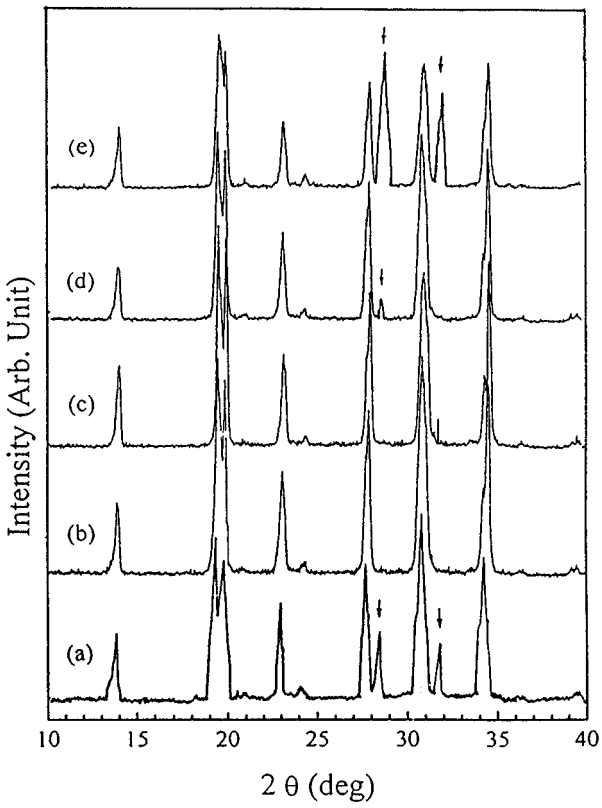

Figure 3 XRD patterns of the air quenched samples. These samples were sintered for 1 h at (a) 1200 °C, (b) 1260 °C, (c) 1300 °C, (d) 1320 °C, and (e) 1360 °C, respectively. Arrows indicate ZrO_2 peaks.

$$ZrO_2 \text{ second phase} + \text{liquid phase} \underset{\text{heating}}{\overset{\text{cooling}}{\rightleftharpoons}} \text{crystalline NASICON}$$

Second, in samples sintered at 1340 °C for 1 h and then cooled to 1260 °C very slowly (at 1 °C/h), followed by air quench to room temperature (Fig. 4c), considerable amount of the ZrO_2 second phase was present, contrary to our expectation.

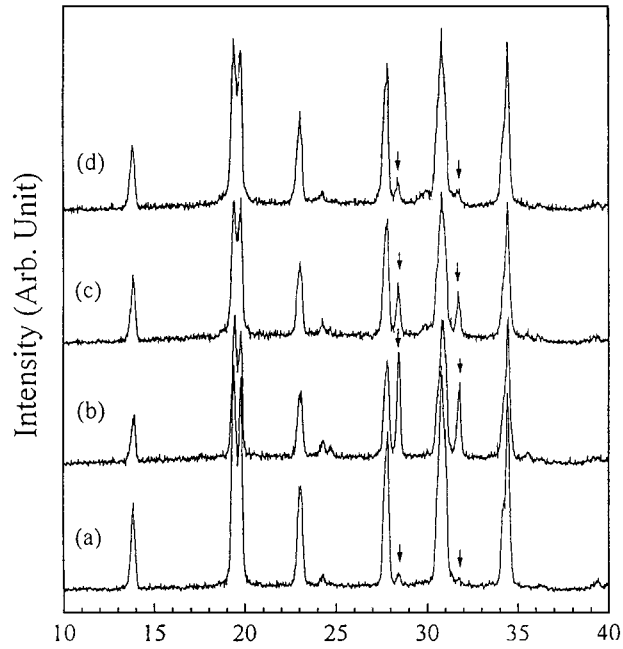

Figure 4 XRD patterns of the samples sintered at 1340 °C for 1 h. These samples were (a) furnace-cooled to room temperature, (b) air quenched to room temperature, (c) cooled to 1260 °C at 1 °C/h followed by air quench, and (d) furnace-cooled to 1260 °C followed by air quench, respectively.

In Fig. 5 are shown the SEM micrographs of the samples sintered at 1340 °C, and then air-quenched to R.T., furnace-cooled to R.T., cooled to 1260 °C at 1 °C/h followed by air quench to R.T., respectively. The general microstructure of the sintered NASICON has been described earlier [24]. The bright, grey, and dark regions in Fig. 5a can be attributed to the ZrO_2 second phase, the crystalline NASICON, and the glass phase, respectively. As shown in Fig. 5b, no ZrO_2 is present in the furnace-cooled samples. This seems to be in good agreement with XRD results in Fig. 4a. The crystalline NASICON present in the air-quenched samples exhibits a considerably sharp interface with the glass phase, whereas in the furnace-cooled samples the interface between the crystalline NASICON and the glass phase

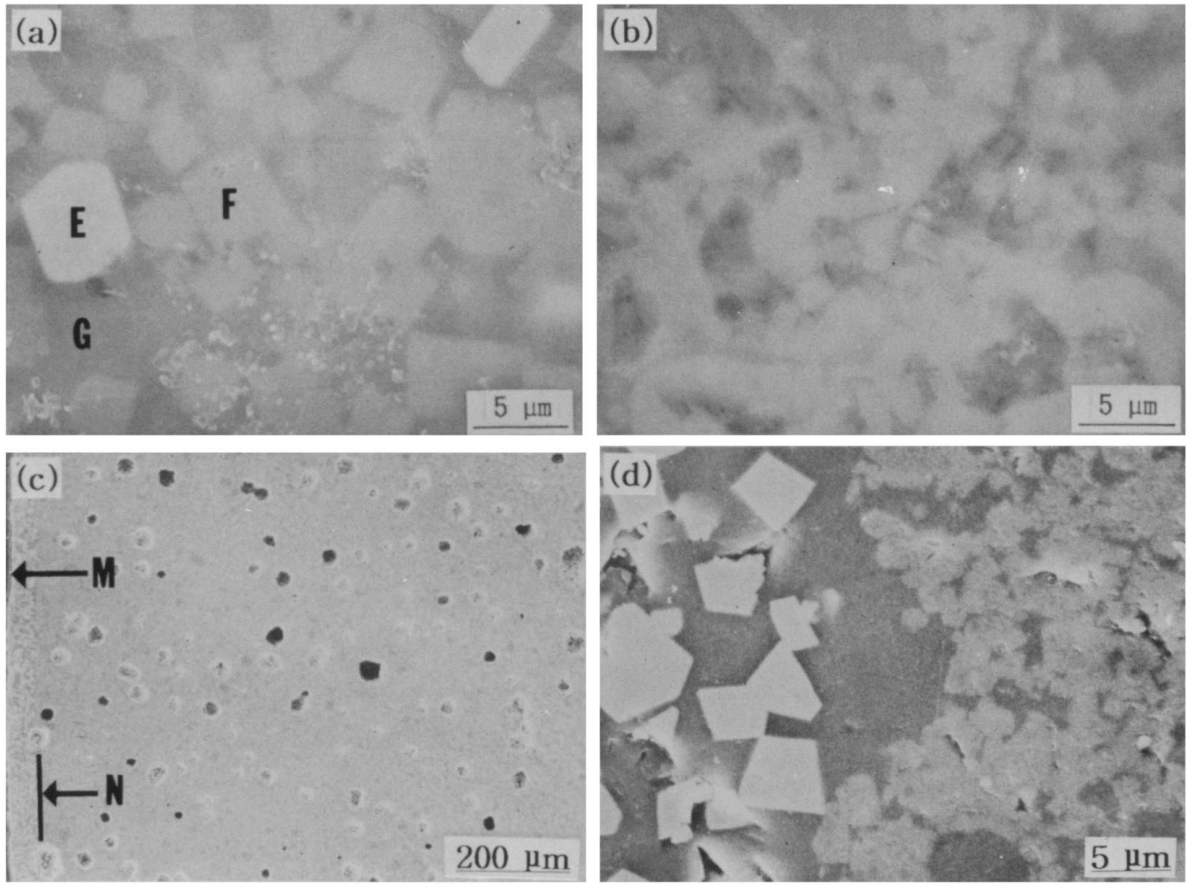

Figure 5 Scanning electron micrographs. The samples were sintered at 1340 °C for 1 h, and then (a) air-quenched to R.T., (b) furnace-cooled to R.T., and (c) cooled at 1 °C/h to 1260 °C followed by air quench to R.T., respectively. In micrograph (a), bright (E), grey (F), and dark (G) regions correspond to the ZrO_2, crystalline NASICON, and glass phases, respectively.

is less clearly seen. During the furnace-cooling process, the ZrO_2 phase, stable at 1340 °C, interacts with the liquid phase to produce the crystalline NASICON. The amount of the crystalline NASICON increased at the expense of the liquid phase during the furnace-cooling process, and consequently the bulk density of the samples would increase.

A large number of ZrO_2 grains is observed locally near the surface of the sintered bodies (Fig. 5c), prepared with a cooling rate of 1 °C/h. The grains seem to be the source of the prominent ZrO_2 peaks in Fig. 4c. EDS results were obtained from a region between the surface (M) and a line denoted with the letter N, and an inner region of the sample, respectively. As is shown in Fig. 6, the amount of Na near the surface region was less than that of the inner region. This deviation from the appropriate chemical formula appears to lead to the absence of crystalline NASICON near the surface, whereas ZrO_2 grains and liquid phase coexist.

In cooling below the congruent point, the total volume of the ZrO_2 second phase would decrease with time for the phase is unstable thermodynamically. Therefore slow-cooling in a temperature range of 1260–1320 °C would be favorable to minimize the amount of the ZrO_2 second phase in sintered NASICON. But increasing cooling time through the temperature range resulted in a decrease in the amount of Na in the sintered bodies. This appears to occur mainly near the surface region. Such a deviation in composition from that of the starting materials prevents the formation of crystalline

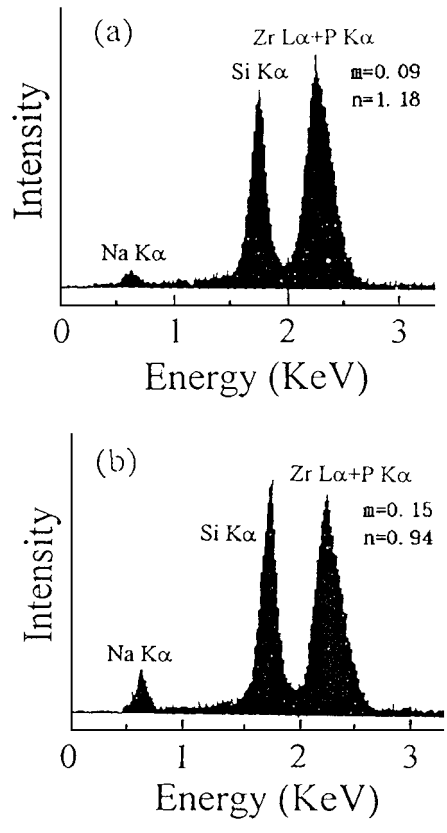

Figure 6 Energy dispersive spectra for the samples shown in Fig. 5c. Spectra (a) and (b) were obtained from a region near surface and an inner region, respectively. Letters *m* and *n* denote the ratios of NaK_α/SiK_α, and ZrL_α/SiK_α, respectively.

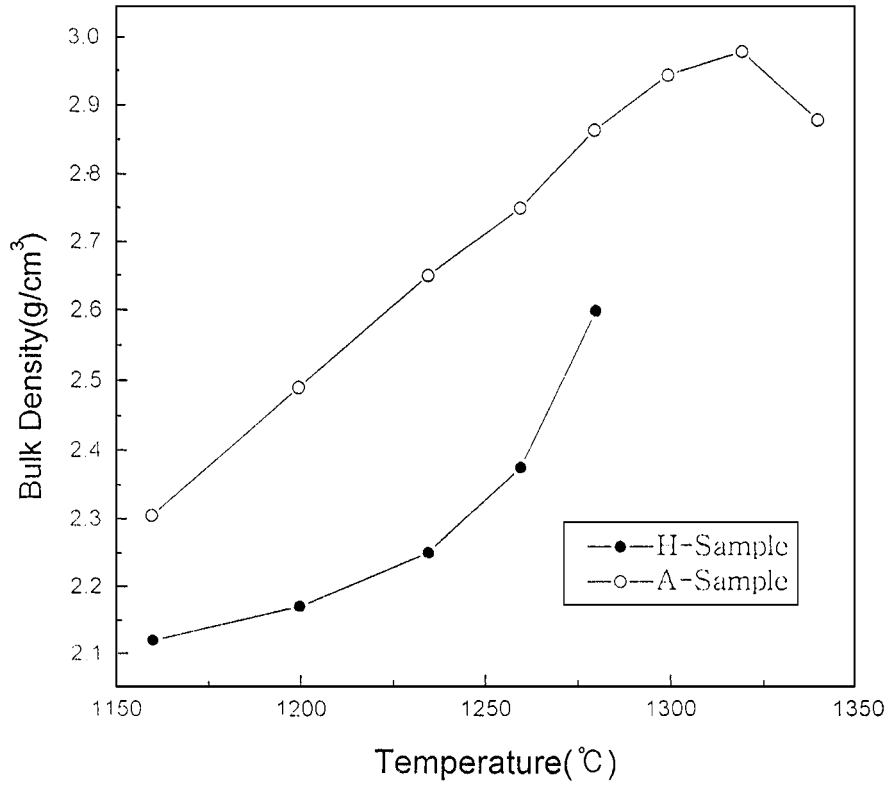

Figure 7 Bulk density of the samples as a function of sintering temperature. The samples were sintered at each temperature for 1 h.

NASICON. This indicates that cooling rate should not be too slow to lose sodium near surface excessively.

3.2. Sintering behavior

3.2.1. Effect of sintering temperature

Fig. 7 shows the density of samples with H- and A-type composition sintered at each temperature for 1 h. The density of H-, and A-type samples increases with raising temperature up to 1280 and 1320 °C, respectively, and the samples were extensively melted above these temperatures. Maximum density for A-type samples is higher than that for H-type samples. In particular, A-type samples have higher melting temperature than H-type samples. These phenomena are believed to occur mainly because A-type samples contain less P (or more Si) than H-type samples [13]. The lower value of the density for H-type samples than for A-type samples in the temperature range can be attributed to the relevant sintering mechanism, and this will be mentioned in the following section.

3.2.2. Effect of sintering time

Shown in Fig. 8 is the density of samples with H- and A-type composition sintered at 1280 and 1300 °C, respectively for up to 18 h. The density of H-type samples reaches its maximum value after 10 h-sintering, and then exhibits little change with time. On the other hand, the maximum density of A-type samples was obtained after 2-h sintering, indicating that densification of A-type samples was achieved much faster than H-type samples. However, the maximum density of A-type samples is lower than that of H-type samples.

Phase diagram of Na_2O-ZrO_2-SiO_2-P_2O_5 relevant to NASICON compounds indicates that a few eutectic reactions between 2 or 3 phases may produce some liquid phase with a composition of corresponding sites at relevant liquidus lines in a temperature range from 900 to 1200 °C [32]. In the calcination process of A-type composition, so-called "hard powder cakes" were produced, while very few of such cakes were observed in the calcined H-type powders. This indicates that much more liquid phases were produced in A-type composition during calcination process than in H-type composition. As a result, more liquid phase is involved in sintering process for A-type than for H-type samples. The densification requires much shorter time in A-type composition than in H-type composition. On the other hand, Such liquid phases remain as a glass phase in the sintered bodies after cooling process. Consequently the relative density of H-type samples is higher than A-type samples. The resultant microstructural features are strongly related with the difference in the electrical characteristics of the two different type samples.

3.3. Electrical characteristics

A frequency range of 10^2 to 4×10^6 Hz was used to measure the ionic conductivity of the sintered NASICON. The dc conductivity was taken as the value of the frequency independent plateau in the σ-f plot [30, 31]. At various conductivity measurement temperatures between room temperature and 300 °C in this investigation, a part of this plateau was observed within the range of experimental frequencies, and dc conductivity at each temperature could be determined from relevant plots. In Fig. 9, a frequency independent region is clearly seen on the curve obtained at 40 °C from a H-type sample sintered at 1280 °C for 8 h. The measured conductivities were ploted over a wide

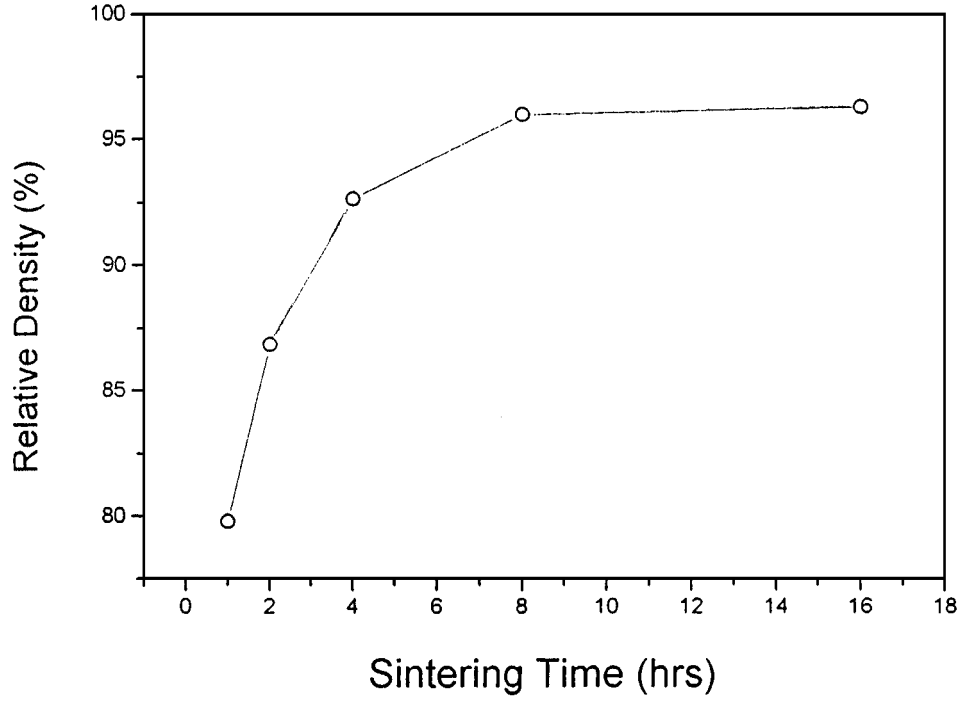

(a)

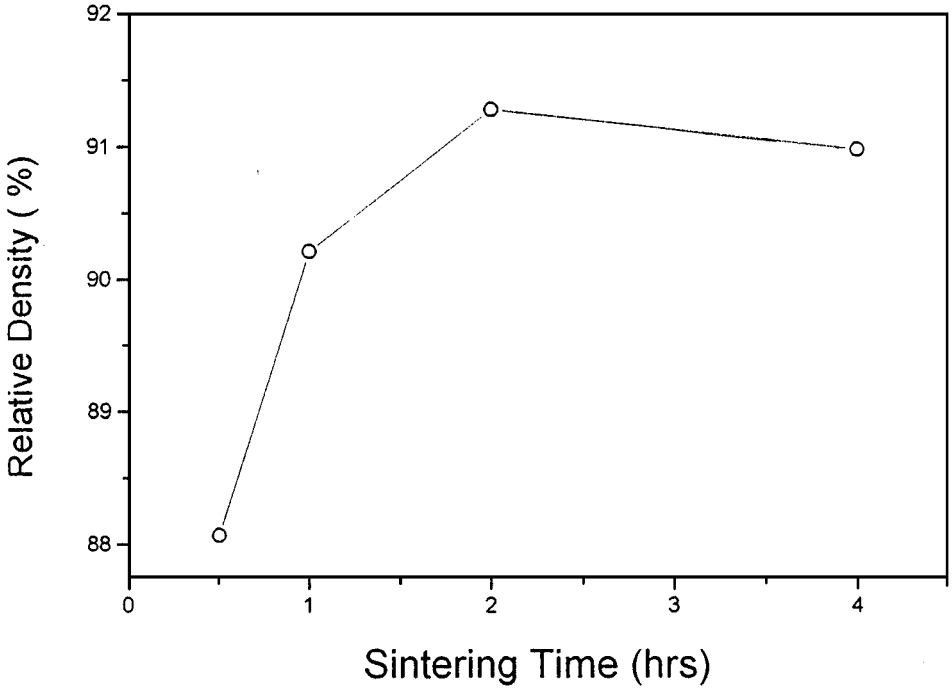

(b)

Figure 8 Relative density of the samples as a function of sintering time. The samples with (a) H-type composition and (b) A-type composition were sintered at 1280 °C and 1300 °C, respectively.

temperature range so that Arrhenius equation could be applicable.

Fig. 10a shows the ionic conductivity measured in a temperature range from room temperature to 300 °C for H-type samples sintered at 1280 °C for 1–16 h, and at 1260 °C for 1 h, respectively. Fig. 10b shows the ionic conductivity in the same measuring temperature range for A-type samples sintered at 1300 °C for 0.5–4 h. Based on the temperature dependency of the ionic conductivity, the migration barrier heights for Na^+ ions were obtained from the slopes in the corresponding log σT vs. $1/T$ plots. In both of the two different type samples (H-, and A-type), a significant change in the migration barrier height occurs at about 200 °C. This change seems to be related with the structural change between monoclininc (C2/c) and rhombohedral (R3c) crystal systems, and is far from the second-order transition suggested by a few research groups [18–21].

In Fig. 10a, H-type samples sintered at 1280 °C for 4–16 h have a similar ionic conductivity, but the samples

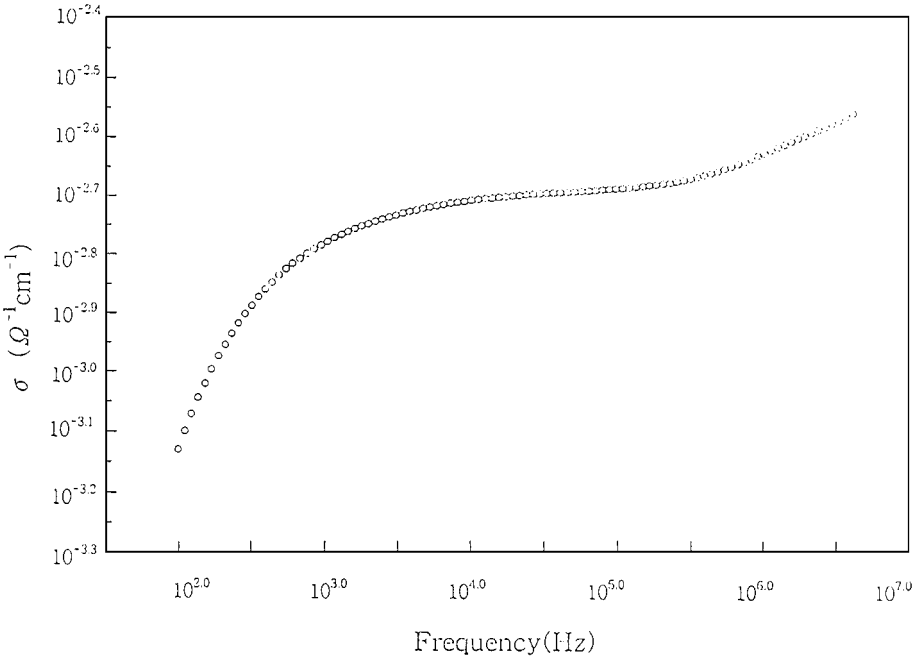

Figure 9 Electrical conductivities for a NASICON compound with H-type composition sintered at 1280 °C for 8 h.

TABLE I Ionic conductivities of superionic conductors

Specimen	σ (ohm^{-1} cm^{-1}) at 300 °C	E (eV)	Reference
Single crystal β-alumina	0.213	0.13	9
Polycrystalline β-alumina	0.08	0.25	9
Polycrystalline β''-alumina	0.2–0.4	0.16–0.22	9
Polycrystalline $Na_{1+x}Zr_2P_{3-x}Si_xO_{12}$	0.2–5.4 × 10^{-4} (x = 0.4 to 2.8)	(0.24–0.32)[a]	2
Na_2O-Ga_2O_3 (Na β-gallate)	0.03	0.27[a]	33
Polycrystalline $Na_3Zr_2PSi_2O_{12}$	0.45	0.07[a] (0.20)[b]	Present data
Polycrystalline $Na_{3.2}Zr_{1.3}Si_{2.2}P_{0.8}O_{10.5}$	0.22	(0.07–0.09)[a] (0.16–0.18)[b]	Present data

[a]The energy barriers were measured at −300 °C.
[b]The energy barriers were measured in a temperature range from room temperature to 200 °C.

sintered at 1260 °C for 1 h, or 1280 °C for 1 h have much lower conductivity than the others. On the other hand, all these samples have the same migration barrier height. The maximum conductivity of H-type samples is 0.45 ohm^{-1} cm^{-1}, while the migration barrier heights for the low and high temperature forms are 0.20 and 0.07 eV, respectively. This suggests that for H-type samples, the migration barrier height is strongly affected by the dominant presence of the crystalline NASICON, while the conductivity is related with the density of the sintered bodies. All the samples therefore seem to have nearly the same crystallinity of NASICON. These values appear to be lower than the results reported previously for similar ionic conductors, as listed in Table I [9, 33]. It is of course necessary to be careful to make a simple direct comparison with other conductors because the physical conditions as well as the preparation techniques are not the same.

In Fig. 10b, A-type samples have the maximum conductivity of 0.22 ohm^{-1} cm^{-1}, half of the corresponding value of H-type samples. For A-type samples, there is little difference in its density with one another, and also no significant difference in conductivity depending on sintering time, compared with the difference seen in H-type samples.

Below −200 °C, the ionic migration barrier height for A-type samples exhibits a range of 0.16–0.18 eV, compared to nearly a single value of 0.20 eV for H-type samples. Such a variation seen in A-type samples seems to be due to their microstructural features; the amount of glass phase in A-type samples is variable depending on its sintering time. The apparent ionic migration barrier height of the samples is the sum of that in the glass phase as well as that in the crystalline NASICON, due to the composite-like microstructure of the samples. Considering that, based on the barrier height for H-type samples with little glass phase, the barrier height of the crystalline NASICON is −0.20 eV below the transition temperature, the migration barrier height for the Na^+ ions in the glass phase is regarded lower than that in the crystalline NASICON. As measurement temperature increases over the transition point (−200 °C), the migration barrier height in the glass phase is higher than that in the crystalline NASICON, resulting in a little higher resistivity, compared to that in H-type samples.

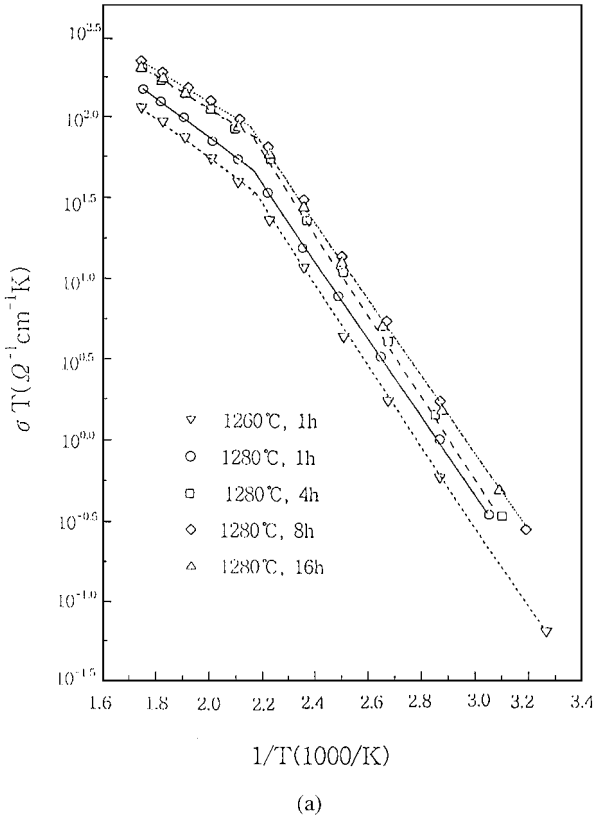

(a)

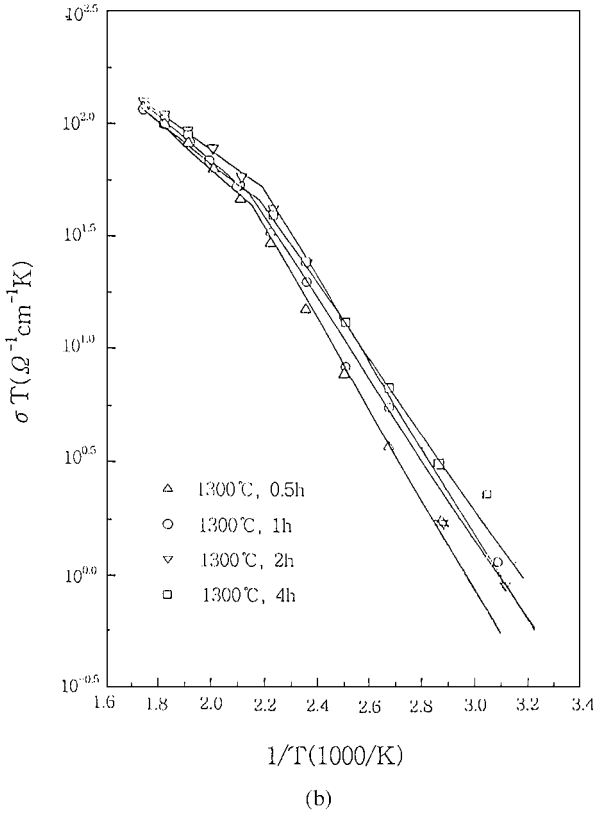

(b)

Figure 10 σT vs. 1000/T for the NASICON compounds. (a) H-type composition. (b) A-type composition.

4. Conclusion

It is essential to choose an appropriate sintering temperature and cooling rate to produce sintered NASICON with less ZrO_2 and higher electrical conductivities. In von Alpen-type NASICON, the ZrO_2 second phase is in thermal equilibrium with the crystalline NASICON and the liquid phase above 1320 °C, but when cooled through 1260–1320 °C, the crystalline NASICON was formed by reaction between the ZrO_2 second phase and the liquid phase. The NASICON compounds sintered above the congruent point should be cooled slow through 1260–1320 °C so that the ZrO_2 second phase could be completely dissolved into the crystalline NASICON. However, cooling rate should not be too slow to lose sodium near surface excessively.

As was expected, denser sintered bodies are favorable for higher electrical conductivity. In our investigation, maximum conductivity of 0.45 ohm^{-1} cm^{-1} was obtained at 300 °C from the sintered NASICON with maximum relative density of 96%. The migration barrier height for Na^+ ions in the glass phase is lower than that in the crystalline NASICON below the transition temperature, but the situation is reversed above the temperature. In the sintered NASICON, the migration barrier height is 0.07–0.09 eV above the transition temperature, and 0.16–0.20 eV below the temperature.

Acknowledgement

The authors acknowledge the financial support for this work by Inha University (1996).

References

1. H. Y-P. HONG, *Mat. Res. Bull.* **11** (1976) 173.
2. J. B. GOODNOUGH, H. Y-P. HONG and J. A. KAFALAS, *ibid.* **11** (1976) 203.
3. J. L. SUDWORTH, in "The Sodium Sulfer Battery," edited by J. L. Sudworth and A. R. Tilley (Chapman and Hall, New York, 1985) p. 5.
4. R. S. GORDON, G. R. MILLER, T. D. HADNAGY, B. J. McENTIRE and T. R. RASMUSSEN, in "Energy and Ceramics," edited by P. Vincenzini (Elsevier, New York, 1980) p. 925.
5. T. MARUYAMA, Y. SAITO, Y. MATSUMOTO and Y. YANO, *Solid State Ion.* **17** (1985) 281.
6. Y. SAITO, T. MARUYAMA and S. SASAKI, *Tokyo Institute of Technology* **9** (1984) 17.
7. S. YAMAGUCHI and A. IMAI, *Ceramics Japan* **27** (1992) 122.
8. *Idem., Ceram. Jpn.* **27** (1992) 122.
9. P. T. MOSELY, in "The Sodium Sulfer Battery," edited by J. L. Sudworth and A. R. Tilley (Chapman and Hall, New York, 1985) p. 19.
10. P. VASHISHITA, J. N. MUNDY and G. P. SHENOY (Elsevier, New York, 1979) p. 45.
11. B. J. McENTIRE, G. R. MILLER and R. S. GORDON, in "Sintering Process," edited by G. C. Kuczynski (Plenum Press, New York, 1980) p. 517.
12. S. FUJITSU, M. NAGAI, T. KANAZAWA and I. YASUI, *Mat. Res. Bull.* **16** (1981) 1299.
13. B. J. McENTIRE, R. A. BARTLETT, G. R. MILLER and R. S. GORDON, *J. Amer. Ceram. Soc.* **66** (1983) 738.
14. K. D. KREUER, H. KOHLER, U. WARBUS and H. SCHULZ, *Mat. Res. Bull.* **21** (1986) 149.
15. J. B. GOODENOUGH, in "Solid Electrolytes," edited by Paul Hagenmuller and W. Van Gool (Academic Press, New York, 1978) p. 393.
16. O. TILLEMENT, J. ANGENAULT, J. C. CONTURIER and M. QUARTON, *Solid State Ion.* **53** (1992) 391.
17. U. VON ALPEN, M. F. BELL and H. H. HOFER, *ibid.* **3/4** (1981) 215.
18. J. P. BOILOT, G. COLLIN and R. COMES, *ibid.* **5** (1981) 307.
19. U. WARHUS, J. MAIER and A. RABENAU, *J. Solid State Chem.* **72** (1988) 113.
20. H. SCHMID, L. C. DeJONGHE and C. CAMERON, *Solid State Ion.* **6** (1982) 57.

21. Ph. COLOMBAN, *ibid.* **21** (1986) 97.
22. H. KOHLER and H. SCHULZ, *Mat. Res. Bull*. **20** (1985) 1461.
23. W. WANG, D. LI and J. ZHAO, *Solid State Ion.* **51** (1992) 97.
24. A. K. KURIAKOSE, T. A. WHEAT, A. AHMAD and J. DIROCCO, *J. Amer. Ceram. Soc.* **67** (1984) 179.
25. R. S. GORDON, G. R. MILLER, B. J. McENTIRE, E. D. BECK and J. R. RASMUSSEN, *Solid State Ion.* **3/4** (1981) 243.
26. A. AHMAD, T. A. WHEAT, A. K. KURIAKOSE, J. D. CANADAY and A. G. McDONALD, *ibid.* **24** (1987) 89.
27. J. J. KIM, T. S. OH, M. S. LEE, J. G. PARK and Y. H. KIM, *J. Mater. Sci.* **28** (1993) 1573.
28. J.-H. CHOY, Y.-S. HAN, Y.-H. KIM and K.-S. SUH, *Jpn. J. Appl. Phys*. **32** (1993) 1154.
29. N.-H. CHO, HEE-BOG KANG and Y.-H. KIM, in Proc. of the 11th Korea-Japan Seminar on New Ceramics, Yongpyeong, Korea, **11** (1994) 435.
30. I. M. HODGE, M. D. INGRAM and A. R. WEST, *J. Amer. Ceram. Soc.* **59** (1976) 360.
31. R. J. GRANT, I. M. HODGE, M. D. INGRAM and A. R. WEST, *ibid.* **60** (1977) 226.
32. E. T. TURKDOGAN and W. R. MADDOCKS, *J. Iron Steel* **172** (1952) 1.
33. S. CHANDRA, "Superionic Solids Principles and Applications" (North-Holland, 1981) p. 17.

Received 30 September 1998
and accepted 24 March 1999